2013 International Nuclear Atlantic Conference - INAC 2013
Recife, PE, Brazil, November 24-29, 2013
ASSOCIAÇÃO BRASILEIRA DE ENERGIA NUCLEAR - ABEN
ISBN: **978-85-99141-05-2**

STRUCTURAL ANALYSIS OF IRRADIATED CROTOXIN BY SPECTROSCOPIC TECHNIQUES

Karina C. de Oliveira, Tamara M. Fucase, Ed Carlos S. e Silva, Bruno B. Chagas, Alisson T. Buchi, Vincent L. Viala, Patrick J. Spencer and Nanci do Nascimento

Centro de Biotecnologia – Instituto de Pesquisas Energéticas e Nucleares (IPEN/CNEN - SP)
Av. Professor Lineu Prestes 2242
05508-000 São Paulo, SP
kcorleto@usp.br

ABSTRACT

Snake bites are a serious public health problem, especially in subtropical countries. In Brazil, the serum, the only effective treatment in case of snake bites, is produced in horses which, despite of their large size, have a reduced lifespan due to the high toxicity of the antigen. Ionizing radiation has been successfully employed to attenuate the biological activity of animal toxins. Crotoxin, the main toxic compound from *Crotalus durissus terrificus* (Cdt), is a heterodimeric protein composed of two subunits: crotapotin and phospholipase A_2. Previous data indicated that this protein, following irradiation process, undergoes unfolding and/or aggregation, resulting in a much lower toxic antigen. The exact mechanisms and structural modifications involved in aggregation process are not clear yet. This work investigates the effects of ionizing radiation on crotoxin employing Infrared Spectroscopy, Circular Dichroism and Dynamic Light Scattering techniques. The infrared spectrum of lyophilized crotoxin showed peaks corresponding to the vibrational spectra of the secondary structure of crotoxin, including β-sheet, random coil, α-helix and β-turns. We calculated the area of these spectral regions after adjusting for baseline and normalization using the amide I band (1590-1700 cm^{-1}), obtaining the variation of secondary structures of the toxin following irradiation. The Circular Dichroism spectra of native and irradiated crotoxin suggests a conformational change within the molecule after the irradiation process. This data indicates structural changes between the samples, apparently from ordered conformation towards a random coil. The analyses by light scattering indicated that the irradiated crotoxin formed multimers with an average molecular radius 100 folds higher than the native toxin.

1. INTRODUCTION

Serum therapy is the only effective treatment for snake-bites. Ophidic antisera are produced by immunization of horses with crude venom. However, snake venoms are, in general, weak immunogens inducing low humoral and cellular immune responses [1-3]. In addition, the high toxicity of snake venoms reduces the useful life of immunized horses, limiting the antisera productivity. Since the antivenoms production affects the lifespan of horses, several methods involving chemical or physical modifications of toxins have been used to detoxify venoms [3,4], including iodination [5-7], photo oxidation [8], X rays irradiation [9], ultraviolet rays [10], treatment with glutaraldehyde [11] and encapsulation of toxins in liposomes [12].

Ionizing radiation, specifically gamma rays, has been employed as a potential process to modify biomolecules, because this method decrease venom toxicity while preserving its immunogenicity, in order to improve antisera production [2,13-17]. Gamma rays alter protein structure by direct process – ionizing radiation interacts directly on target biomolecules and indirectly – the products generated by water radiolysis interact with target molecules [13,18]. Indirect process is the main form of action, representing approximately 80% of the total

effect. In addition, the main species formed, with yields respectively, for 100 eV of absorbed energy, are:

$$H_2O \rightarrow 2.7\ e^-_{aq.} + 0.45\ H_3O^+ + 3.2\ OH\bullet + 0.6\ H^+ + 0.45\ H_2 + 0.7\ H_2O_2 \quad [19]$$

Crotoxin, the major heterodimeric toxin of the venom of the South American rattlesnake *Crotalus durissus terrificus*, is a potent β-neurotoxin that possesses phospholipase A_2 (PLA_2) activity and exerts a lethal action by blocking neuromuscular transmission. The crotoxin acts primarily by causing a triphasic change (depression, facilitation and final blockage) of acetylcholine release at the motor nerve terminal. Secondarily, crotoxin induces a postsynaptic blockage of neuromuscular by stabilizing a desensitized state of the nicotinic receptor [16,20,21]. Crotoxin consists of a noncovalent association of a basic and weakly toxic PLA_2 subunit, CB, with a small acidic, nonenzymatic, and nontoxic subunit, CA. Purified CB exhibits weak lethality but becomes over 100 times more potent with the addition of the acidic component [22]. Moreover, the CA subunit is a natural inhibitor of the catalytic and anticoagulant activity of CB [23,24].
Numerous studies have shown that the crotoxin heterodimer, as well as its CB subunit, display a number of other pharmacological effects in addition to neurotoxicity, including local and systemic myotoxicity, necrosis of skeletal muscle and myoglobinuria [25-27]. Furthermore, crotoxin exhibits a preferential cytotoxic activity against various types of tumor cells and is more cytotoxic to cell lines that express high levels of epidermal growth factor receptors [28-31]; accordingly, it is used in the treatment of carcinomas [32,33].
In this work we studied irradiation effects on crotoxin structure by Infrared Spectroscopy (FTIR), Circular Dichroism (CD) and Dynamic Light Scattering (DLS) techniques.

2. MATERIAL AND METHODS

2.1. Venom

Crude air-dried venom from *Crotalus durissus terrificus* was supplied by CEVAP (Botucatu – SP – Brazil).

2.2. Crotoxin Purification

Crude venom was dissolved in 200 mM, pH 3.0 ammonium formiate buffer, centrifuged at 14,000 g for 5 minutes to remove insoluble material, and fractionated on a 1.6x70 cm Superdex G-75 column (Pharmacia-Biotech), equilibrated in the same buffer at 0.5 mL/min. The absorbance of the eluate was monitored at 280 nm. The fraction corresponding to crotoxin was pooled and refractionated on a Mono Q column – 5 mL (Pharmacia Biotech AB), equilibrated in buffer A (50 mM, TRIS/HCl, pH 8.2). Buffer B was identical to buffer A, except by 2 M NaCl. After an initial wash with 5% buffer B, elution was started with a linear gradient up to 30% buffer B. The column was regenerated with 100% buffer B followed by buffer A to wash. The fraction was pooled and then desalted by dialysis and lyophilized.

2.3. Crotoxin Irradiation

Purified toxin was dissolved in 0.15 M NaCl solution to a final concentration of 2.0 mg/mL and irradiated with 2.0 kGy using gamma rays from a ^{60}Co source (Gammacell 220 Canada), in the presence of O_2, at room temperature and with a dose rate of 1.2 kGy/h.

2.4. Fourier Transform Infrared Spectroscopic Analysis (FTIR)

To analyse the secondary structure from native and irradiated crotoxin, the vibrational spectra were obtained by FTIR. The samples were analyzed from 650 to 2,000 cm^{-1}, with a resolution of 4 cm^{-1} and 120 scans. The spectra were corrected at base line and normalized in terms of amide band I area to minimize the homogeneity variation of samples. The area of each band was calculated based in literature.

2.5. Circular Dichroism Spectroscopy (CD)

Circular dichroism spectrocopy was used to quantify the secondary structure of native and irradiated toxin. This analysis was realized with 500 µL of each sample in quartz cell (0.1 mm path length). The acquisition region was between 195 nm and 250 nm. The temperature throughout the experiment was kept at 20 ºC.

2.6. Dynamic Light Scattering Analysis (DLS)

The principle of DLS is based on the scattering of light by moving particles. Crotoxin at 2 mg/ml in PBS, in both native and irradiated states, was analyzed with an equipment developed by the group of Dr. C. Betzel (University of Hamburg).

3. RESULTS

Figure 1 show us differences between the native (red line) and irradiated (blue line) crotoxin spectra in the infrared region. The amides areas are highlighted.

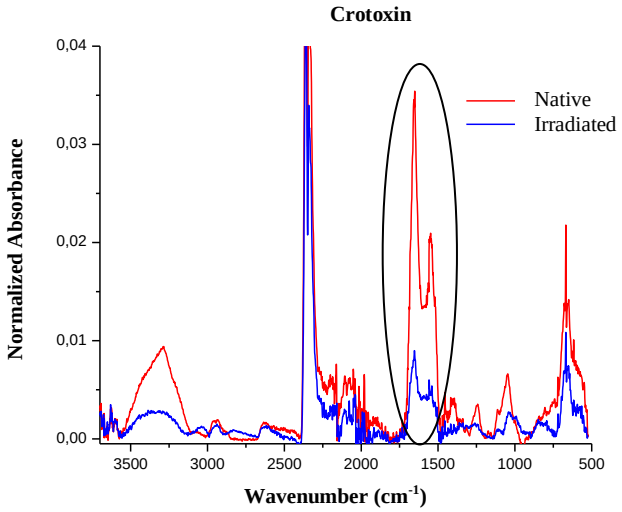

Figure 1: Absorbance spectra of native (red line) and irradiated (blue line) crotoxin.

Figure 2 illustrates the relative amounts of secondary structure elements of the native and irradiate protein. A significant decrease in β-turns and α-helix and an apparent increase of β-sheet was observed after irradiation.

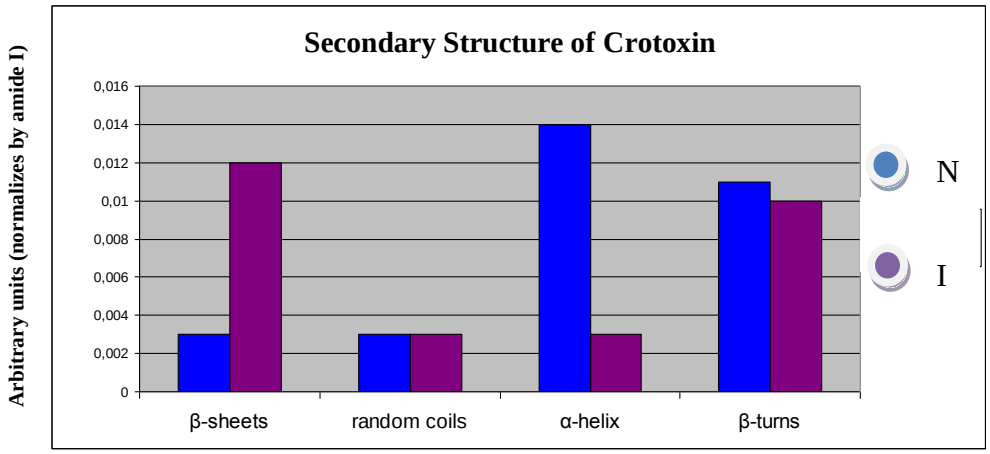

Figure 2: Relative amounts of secondary structure elements of the native (blue line) and irradiate (purple line) crotoxin.

Figure 3 illustrates the CD spectra of native and irradiated crotoxin. Our data indicate the secondary structure modifications of crotoxin, following irradiation, confirming the FTIR data. The major transition regions were in the range between 195 and 200 nm and around 216 nm (β-sheet). The characteristic regions of α-helix exhibit variations too (~208 – 210 nm and ~220 nm).

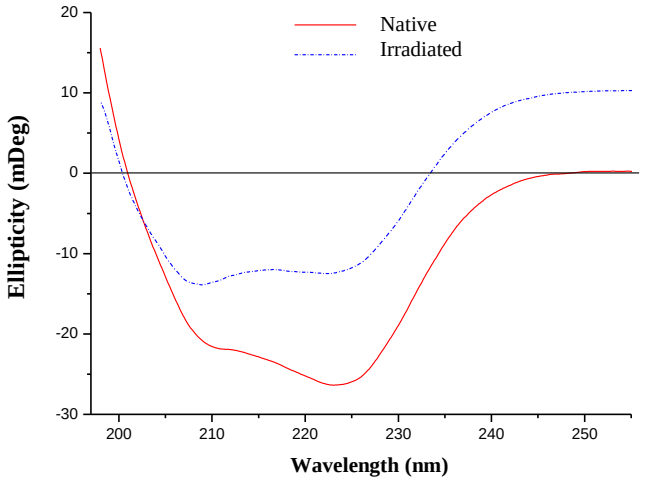

Figure 3: CD spectra of native (red line) and irradiated (blue line) crotoxin. Concentration of toxin was 400 µg/mL, in phosphate buffer, 25 mM, pH 7.2.

The DLS analysis indicates significant alterations of the dispersivity of the protein, with an increase of the molecular size after irradiation Figure 4 illustrates the molecular radius distribution of crotoxin molecules in the native state. The major region is between 1 and 10 nm. There is a direct correlation between molecular radius and mass of the protein, and our data clearly indicate an increase in molecular radius (aggregation).

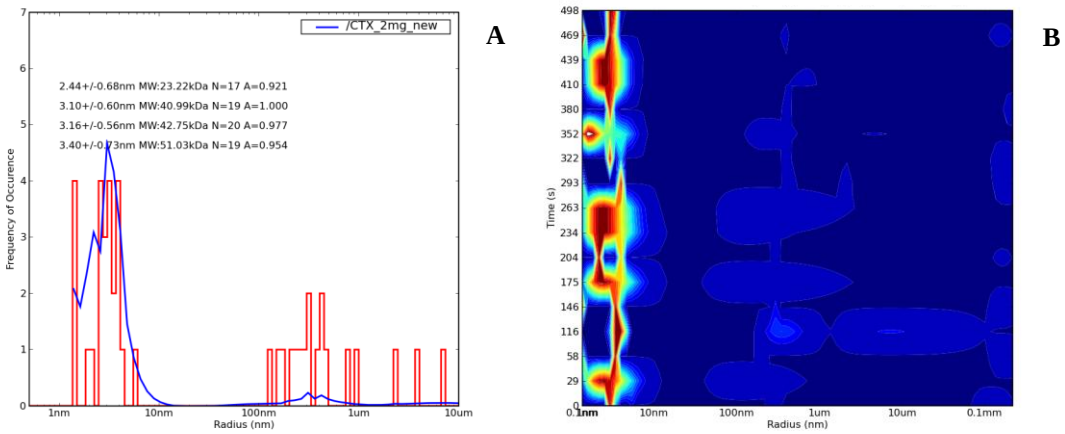

Figure 4: DLS analysis of crotoxin in the native state (A); DLS analysis of radius distribution of toxin in the native state (B).

Figure 5 exhibits the same approach of DLS analysis, but to irradiated crotoxin. The major region in this case is between 100 and 1000 nm. Therefore we have observed an important difference compared native and irradiated forms.

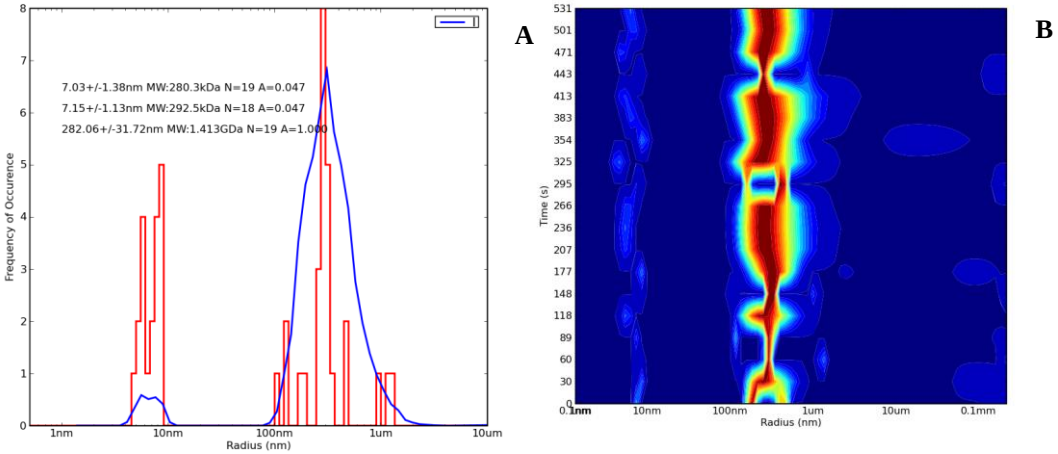

Figure 5: DLS analysis of crotoxin in the irradiated state (A); DLS analysis of radius distribution of toxin in the irradiated state (B).

4. DISCUSSION AND CONCLUSIONS

Radiation has been successfully employed to detoxify snake venoms and toxins, however the effects of radiation on the toxins are not yet fully characterized.

Following purification (data not shown), crotoxin, in solution, was irradiated with 2 kGy.

Protein irradiation leads to a wide array of modifications in the molecule structure, ranging from simple ionization up to drastic changes in primary, secondary, tertiary and quaternary structures. Such alterations are related to the loss of biological activity and also interfere with the immunological properties of irradiated toxins [34].

It is well known that the determination of the structural conformation can provide valuable insights about the biological function of a protein [35]. Considering that the major

modifications of proteins submitted to irradiation are structural, investigating these alterations could help to clarify the mechanisms by which the toxic and immunological properties of irradiated toxins are modified.

FTIR vibrational spectra results from the absorption of energy by vibrating chemical bonds (primarily stretching and bending motions). Characteristic groups of atoms give rise to vibrational bands near the same frequency regardless of the molecule in which they are found. The precise wavenumbers of bands within this range depend on inter and intramolecular effects, including peptide-bond angles and hydrogen-bonding patterns. Thus, vibrational spectra can be used to estimate the secondary structure of proteins by inspection of the frequencies at which the amide bonds absorb infrared radiation. In practice, the amide I band in FTIR is primarily used to assign secondary structures to proteins [35-37].

In figure 1, well defined peaks are observed in the region corresponding to the amide 1 band for the native toxin. For the irradiated sample, these peaks are significantly less intense and poorly defined, suggesting alterations in the secondary structure of the molecule.

Also, the region between 3500 and 3200 cm^{-1} displayed evident differences. Although this region of the spectrum is not relevant for secondary structure studies, it is worth noting that the wavenumber around 3500 cm^{-1} corresponds to O-H bonds of hydroxyl groups, while the bands around 3200 cm^{-1} can be ascribed to N-H bands from amide groups [37]. Proteins are rich in –OH and –NH groups, which form a strong network of intra-molecular bonds. This is one of the major forces that drives protein folding. Thus, the FTIR spectra indicate that crotoxin, after irradiation, suffered severe structural modifications.

Figure 2 reveals that, for the native protein, α-helix is the most abundant structural element, with 45.2% of the total. Crotoxin also presented a fair amount of β-turns (35.5%). Following irradiation, an increase of β-sheets, from 9.7% to 42.8% and consequent decrease of α-helix, from 45.2% to 10.7% was observed. Apparently, random coils and β-turns were not affected. It is noteworthy that our experimental data are very close those obtained by Hanley (1979) [38], Aird, et al. (1989) [39] and the protein databank [40].

Circular dichoism is observed when molecules absorb left and right circularly polarized light to different extents. The amide chromophore of peptide bond in proteins dominates the CD spectrum below 250 nm. In an α-helical protein, a negative band near 222 nm is observed due to the strong hydrogen-bonding environment of this conformation. This transition is relatively independent of the length of the helix. A second transition at 190 nm is split into a negative band near 208 nm and a positive band near 192 nm. Both bands are reduced in intensity in short helices. The CD spectra of β-sheets display a negative band near 216 nm, a positive band between 195 and 200 nm, and a negative band near 175 nm [35].

The CD spectra (Figure 3) clearly indicate differences between native and irradiated crotoxin. The signal corresponding to helical conformation (222 nm) decreased around 50% after irradiation. On what refers to β-sheet, the region around 216 nm indicated significant differences between native and irradiated toxins, with an increase of this structure in the sample Hanley (1979) [38] observed that, when studied separately, the crotoxin subunits displayed different values on what refers to secondary structure elements than when the two subunits are complexed, with the total amount of helical structures being lower when the subunits are separated while the β-sheets are substantially higher when the subunits are dissociated. According to the structural data available in the Protein Data Bank (PDB), the CB2 isoform of the basic subunit of crotoxin has 50% of α-helix, with 62 residues forming helixes while β-sheet represent only 9% of the structure. Another crotoxin isoform, CB1 presents 45% of α-helix, and only 3% of β-sheet. Thus, the presence of crotoxin isoforms in the venom may impair a precise quantification of structural elements, considering that, in the present work, no attempt was done to isolate a specific isoform.

The foundation of DLS is based on the scattering of light by moving particles. The earliest form of the experiment involved the measurement of the very tiny Doppler shifts in the scattered laser light due to the presence of this motion [41].
The hydrodynamic diameter of a non-spherical particle is the diameter of a sphere that has the same translational diffusion speed as the particle. If the shape of a particle changes in a way that affects the diffusion speed, then the hydrodynamic size will change. The conformation of proteins is usually dependent on the exact nature of the dispersing medium. Factors that influence the protein hydrodynamic sizes are the molecular mass of the molecule, the shape of conformation of the molecule and also whether the protein is in its native or folded state [42].
Our DLS data (Figures 4 and 5) indicate significant differences between the molecular radius of native and irradiated crotoxin. Figure 4a shows that for the native toxin, most of the signal was between 1 and 10 nm. For the irradiated protein, the molecular radius went up to 100 to 1000 nm, clearly indicating aggregation. According to these data, an average molecular mass of 23 kDa was obtained for the native toxin, which is in complete agreement with the molecular mass deduced from the protein sequence. Other molecules were detected with calculated masses around 41-51 kDa, suggesting that the toxin might dimerize spontaneously in solution.
For the irradiated samples, the average calculated mass was around 1.5 GDa, suggesting the formation of large protein aggregates. This fact is conceivable, considering that radiation promotes several structural alterations and that these changes may lead to oligomers formation.
It should be emphasized that protein irradiation is a probabilistic event, meaning that the observations here presented are only an average of what occurs with toxin solutions submitted to irradiation. Thus, such data must be interpreted with caution, always considering that several conformational states coexist in an irradiated protein sample, ranging from insoluble aggregates to intact molecules.

ACKNOWLEDGMENTS

We are grateful to CEVAP (Botucatu - SP) for providing the venom and to Dr. Christian Betzel for DLS analysis.
Financial support: CAPES

REFERENCES

1. Magalhães, R.A.; Ribeiro, M.M.F.; Rezende, N.A.; Amaral, C.F.S. Rabdomiólise secundária a acidente ofídico crotálico (*Crotalus durissus terrifucus*). *Rev. Inst. Med. Trop.* São Paulo, **Vol. 28**, pp. 28-33 (1986).
2. Souza, F.A.D.; Spencer, P.J.; Rogero, J.R.; Nascimento, N.; Pai-Silva, M.D.; Gallacci, M. ^{60}Co gamma irradiation prevents *Bothrops jararacussu* venom neurotoxicity and myotoxicity in isolated mouse neuromuscular junction. *Toxicon*, **Vol. 40**, pp. 1101-1106 (2002).
3. Oussedik-Oumehdi, H.; Laraba-Djebari, F. Irradiated *Cerastes cerastes* Venom as a Novel Tool for immunotherapy. *Immunopharmacology and Immunotoxicology*, **Vol. 30**, pp. 37-52 (2008).
4. Phisalix, L.D.; Bertrand, G. Sur la propriété antitoxique du sang des animaux vaccinés contre le venin di vipère. *C. R. Acad. Sci.*, **Vol. 118**, pp. 356-358 (1894).

5. Heneine, I.F.; Lahmann, W.M.; Rocha, O.A. A toxoid prepared for cholera toxin by iodination. *Braz. J. Med. Biol. Res.*, **Vol. 25**, pp. 913-917 (1992).
6. Daniel, J.P.; Heneine, L.D.G.; Tavares, C.A.P.; Nascimento, M.C.S.; Heneine, I.F. Generation of protective immune sera by *C.d.terrificus* venom detoxified by controlled iodination. *Braz. J. Med. Biol. Res.*, **Vol. 20**, pp. 713-720 (1987).
7. Bicalho, R.X.; Rocha, O.A.; Heneine, L.G.D.; Magalhães, A.; Heneine, I.F. The effect of stepwise iodination on biological properties of *Bothrops jararaca* venom. *Toxicon*, **Vol. 28(2)**, pp. 171-179 (1990).
8. Shortt, H.E.; Malllick, S.M.K. Detoxication of snake venoms by the photodynamic action of methylene blue. *Indian J. Med. Res.*, **Vol. 22**, pp. 529-536 (1935).
9. Flowers, H.H. The effects of X-irradiation on the biological activity of cottonmouth moccasin (*Ancistrodon piscivorus*) venom. *Toxicon*, **Vol. 1**, pp. 131-136 (1963).
10. Tejasen, P.; Ottolenghi, A. The effect of ultraviolet light on the toxicity and the enzymatic and antigenic activities of snake venom. *Toxicon*, **Vol. 8**, pp. 225-233 (1970).
11. Guidolin, R.; Dias da Silva, W.; Higashi, H.G.; Caricati, C.P.; Lima, M.L.S.R.; Morais, J.F.; Pinto, J.R.; Marcelino, J.R. Hiperimunização de cavalos soroprodutores com venenos botrópico e crotálico tratados por glutaraldeído. *Mem. Inst. Butantan*, **Vol. 51**, pp. 85-90 (1989).
12. Freitas, T.Y.; Frézard , F. Encapsulation of native crotoxin in liposomes: a safe approach for production of antivenom and vaccination against *Crotalus durissus terrificus* venom. *Toxicon*, **Vol. 35**, pp. 91-100 (1997).
13. Casare, M.S.; Patrick, J.S.; Campos, L.A.; Nascimento, N. Study of gamma-radiation effects on crotamine and crotoxin. *Journal of Radioanalytical and Nuclear Chemistry*, **Vol. 269**, pp. 571-577 (2006).
14. Murata, Y. Efeitos da radiação gama no veneno de *Crotalus durissus terrificus*. 1988. Dissertação (Mestrado) – Instituto de Pesquisas Energéticas e Nucleares, São Paulo.
15. Nascimento, N.; Seebart, C.S.; Francis, B.; Rogero, J.R.; Kaiser, I.I. Influence of ionizing radiation on crotoxin: biochemical and immunological aspects. *Toxicon*, **Vol. 34(1)**, pp. 123-131 (1996).
16. Gallacci, M.; Nunes, E.C.; Moreira, E.G.; Nascimento, N.; Rogero, J.R.; Vassilieff, V.S. Reduction of crotoxin-induced neuromuscular blockage by gamma radiation. *Toxicon*, **Vol. 36**, pp. 941-945 (1998).
17. Gallacci, M.; Nascimento, N.; Rogero, J.R.; Vassilieff, V.S. Influence of temperature upon effects of crotoxin and gamma-irradiated crotoxinat rat neuromuscular transmission. *Toxicol. Lett.*, **Vol. 114**, pp. 77-80 (2000).
18. Butler, J.; Hoey, B.M.; Swallow, A.J. Radiation chemistry. *Annu. Rep. Prog. Chem.*, **Vol. 83**, pp. 129-175 (1987).
19. Butler, J.; Land, E.J.; Swallow, A.J. Chemical mechanisms of the effects of high energy radiation on biological systems. *Radiat. Phys. Chem.*, **Vol. 24**, pp. 273-282 (1984).
20. Slotta C.H. & Fraenkel-Conrat, M. Purificação e cristalização do veneno da cobra cascavel. *Mem. Inst. Butantan*, **Vol. 12**, pp. 505-513 (1938).
21. Hawgood, B.J.; Smith, J.W. The mode of action at the mouse neuromuscular junction of the phospholipase A-crotapotin complex isolated from venom of the South American rattlesnake. *Br. J. Pharmacol.*, **Vol. 61**, pp. 597-606 (1977).
22. Hendon, R.A. & Fraenkel-Conrat, H. Biological roles of the two components of crotoxin. *Proc. Natl. Acad. Sci. USA*, **Vol. 68**, pp. 1560-1563 (1971).

23. Faure, G. Different protein targets for snake venom phospholipases A_2. In *Toxines et recherches biomédicales. SFET collection, "Recontres en toxinologie"*, pp. 305-313 (2002).
24. Faure, G.; Gowda, V.T.; Maroun, R. Characterization of a human coagulation factor Xa-binding site on phospholipases A_2 from *Viperidae* snake venom by affinity bindings studies and molecular bioinformatics. *BMC Struct. Biol*. **Vol. 7**, pp. 82 (2007).
25. Gopalakrishnakone, P.; Hawgood, B.J. Morphological changes induced by crotoxin in murine nerve and neuromuscular junction. *Toxicon*. **Vol. 22**, pp. 791-804 (1984).
26. Mebs, D.; Ownby, C.L. Myotoxic components of snake venom: their biochemical and biological activities. *Pharmacol. Ther*. **Vol. 48**, pp. 223-236 (1990).
27. Gutierrez, J.M.; Ponce-Soto, L.A.; Marangoni, S.; Lomonte, B. Systemic and local myotoxicity induced by snake venom group IIA phospholipases A_2: comparison between crotoxin, crotoxin B and Ly49 PLA_2 homologue. *Toxicon*. **Vol. 51**, pp. 80-92 (2008).
28. Costa, L.A.; Miles, H. Araujo, C.E.; Gonzales, S.; Villarrubia, V.G. Tumor regression of advanced carcionomas following intra- and /or peritumoral inoculation with VRCTC-310 in humans: preliminary report of two cases. *Immunipharmacol. Immunotoxicol.* **Vol. 20**, pp. 15-25 (1998).
29. Donato, N.J.; Martin, C.A.; Perez, M.; Newman, R.A.; Vidal, J.C.; Etcheverry, M. Regulation of epidermal growth factor receptor activity by crotoxin, a snake venom phospholipases A_2 toxin: a novel growth inhibitory mechanism. *Biochem. Pharmacol.* **Vol. 51**, pp. 1535-1543 (1996).
30. Rudd, C.J.; Visckatis, L.J.; Vidal, J.C.; Etcheverry, M.A. In vitro comparison of cytotoxic effects of crotoxin against three human tumors and a normal human epidermal keratinocyte cell line. *Invest. New Drugs*. **Vol. 12**, pp. 183-184 (1994).
31. Yan, C.H.; Yang, Y.P.; Qin, Z.H.; Gu, Z.L.; Reid, P.; Liang, Z.Q. Autophagy is involved in cytotoxic effects of crotoxin in human breast cancer cell line MCF-7 cells. Acta Pharmacol. Sin. Vol. 28, pp. 540-548 (2007).
32. Cura, J.E.; Blanzaco, D.P.; Brisson, C.; Cura, M.A.; Carbol, R.; Larrateguy, L. Phase I and pharmacokinetics study crotoxin (cytotoxic PLA2 NSC-624 244) in patients with advanced cancer. *Clin. Cancer Res*. **Vol. 8**, pp. 1033-1041 (2002).
33. Faure, G.; Xu, H.; Saul, F.A. Crystal Structure of Crotoxin Reveals Key Residues Involved in the Stability and Toxicity of this Potent Heterodimeric β-Neurotoxin. *Journal of molecular Biology*. **Vol. 412**, pp.176-191 (2011).
34. Grosh, D.S. & Hoopywood, L.E. *Biological effects of radiation*. 2nd ed., Academic Press: New York, 1979.
35. Peltron, J.T. & McLean, L.R. Spectroscopic Methods for Analysis of Protein Secondary Structure. *Anal. Biochem.* **Vol. 227**, pp. 167-176 (2000).
36. Kong, J.; Yu, S. Fourier Transform Infrared Spectroscopic Analysis of Protein Secondary Structures. *Acta Biochim. Biophys. Sin.* **Vol. 39(8)**, pp. 549-559 (2007).
37. Beekes, M.; Lasch, P.; Naumann, D. Analytical applications of Fourier transform-infrared (FT-IR) spectroscopy in microbiology and prion research. *Vet. Microbiol***. Vol. 123(4)**, pp. 305-319 (2007).
38. Hanley, M.R. Conformation of the Neurotoxin Crotoxin Complex and Its Subunits. *Biochemistry*. **Vol. 18(9)**, pp. 1681-1688 (1979).
39. Aird, S.D.; Steadman, B.L.; Middaugh, C.R.; Kaiser, I.I. Comparative spectroscopic studies of four crotoxin homologs and their subunits. *Biochem. Biophys. Acta*. **Vol. 997**, pp. 211-218 (1989).
40. PROTEIN DATA BANK. Banco de dados. Disponível em:< http://www.rcsb.org/pdb/home/home.do> (2013).

41. Dalgleish, D.G.; Hallett, F.R. Dynamic light scattering: applications to food systems. *Food Research International*. **Vol. 28(3)**, pp. 181-193 (1995).
42. Arzensek, D. Dynamic light scattering and application to proteins in solutions. Seminar – 4th year. University of Ljubljana, Faculty of Mathematics and Physics (2010).